Electronic equalization of 10 Gbit/s upstream signals for asynchronous-modulation and chromatic-dispersion compensation in a high-speed centralized supercontinuum broadband-light-source WDM-PON

Jian Zhao* and Lian-Kuan Chen

Department of Information Engineering, The Chinese University of Hong Kong, Shatin, New Territories, Hong Kong Special Administrative Region, China
*Corresponding author: jzhao2@ie.cuhk.edu.hk

We propose maximum likelihood sequence estimation (MLSE) for upstream signal detection in a high-speed centralized supercontinuum broadband-light-source (SC-BLS) wavelength-division-multiplexing passive optical network (WDM-PON). Upstream pulse carriers are produced by a SC-BLS at the central office (CO), modulated by 10 Gbit/s upstream data at optical network units (ONUs), and finally detected by MLSE at the CO. MLSE effectively compensates the impairments from (1) asynchronous modulation of upstream pulse carriers at ONUs; and (2) chromatic dispersion (CD) in the fibers. Compared to the conventional method using alignment monitors at ONUs for upstream modulation synchronization and all-optical components for CD compensation, the proposed method features significant cost saving, lower power requirement for upstream signals, and lower operation complexity for ONUs in the SC-BLS WDM-PON. © 2007 Optical Society of America

OCIS codes: 060.2330, 060.4250.

1. Introduction

The wavelength-division-multiplexing passive optical network (WDM-PON) is one of the most promising technologies to meet the increasing bandwidth demand from enterprises and households [1–3]. A centralized broadband light source (BLS) at the central office (CO), used for producing upstream carriers by spectrum slicing, is desirable in a WDM-PON because such source features well-controlled wavelength spacing and management-cost reduction by eliminating wavelength-specific transmitters at optical network units (ONUs). Supercontinuum (SC) generation by feeding a pulse train into an SC nonlinear fiber is an effective way to obtain a BLS with more than 100 high-quality and well-wavelength-managed upstream carriers [4]. A broadband SC spectrum also has a higher optical signal-to-noise ratio (OSNR) compared to that generated by a conventional BLS such as a light-emitting diode. Therefore, it can support a larger number of channels with a higher data rate (10 Gbit/s) and a longer transmission distance [3]. In a SC-BLS WDM-PON, to achieve proper upstream data modulation, it is essential to locate the pulse peak of the upstream carriers in the middle of the upstream data bit slot. However, because the optical pulse carriers are generated at the CO but modulated at ONUs, the synchronization between upstream pulse carriers and upstream data is difficult. Furthermore, chromatic dispersion (CD) becomes an important issue for upstream signals due to the high transmission data rate of 10 Gbit/s and wide spectral width, as wide as the bandwidth of the arrayed waveguide grating (AWG) for channel slicing. Therefore, both CD compensation components and alignment monitors at ONUs for upstream modulation synchronization are required. As a result, the operation complexity of ONUs as well as the cost of the network are increased.

Recently, electronic impairment compensation has attracted considerable interest because of its significant cost saving and adaptive compensation capability [5,6]. The implementation of 10 Gbit/s maximum likelihood sequence estimation (MLSE) has been reported [7]. In this paper, we propose MLSE for upstream signal detection in a SC-BLS WDM-PON. We analytically show that MLSE at the CO can effectively compensate the impairments from not only CD in the fibers but also asynchronous upstream modulation at ONUs. Compared to the conventional method, by using alignment monitors at ONUs and all-optical CD compensation components, the proposed method features significant cost saving, lower power requirement for upstream signals, and lower maintenance cost for ONUs in the SC-BLS WDM-PON.

2. Principles of the Proposed Scheme

Figure 1 shows the general architecture of the SC-BLS WDM-PON [3]. A C-band 10 Gbit/s SC light source and L-band 10 Gbit/s distributed feedback (DFB) transmitters are located at the CO for the generation of upstream carriers and downstream signals, respectively. The SC spectrum is generated by launching an optical pulse train from a mode-locked fiber laser (MLFL) into a nonlinear SC fiber. The broadened SC spectrum is then filtered by a C-band optical bandpass filter (OBPF) and combined with the downstream signals by a C/L band combiner. The combined upstream carriers and downstream signals are fed into a piece of single-mode fiber (SMF) with CD compensation by a dispersion compensating fiber (DCF) in conventional architecture [3]. At the remote node (RN), the upstream carriers and downstream signals are separated by a C/L band splitter, and demultiplexed by C-band and L-band demultiplexers (DEMUXs), respectively. Each ONU consists of a receiver for downstream signal detection and a synchronized modulator for upstream data modulation. The 10 Gbit/s upstream signals from ONUs are multiplexed by a C-band multiplexer (MUX) at the RN and sent back to the CO, where they are demultiplexed for detection. In this WDM-PON with colorless ONUs, both downstream and upstream signals can operate at 10 Gbit/s. In principle, SC-BLS can generate more than 100 high-quality upstream carriers by spectrum slicing. However, CD becomes an issue for upstream signals due to the high data rate of 10 Gbit/s and wide spectral width, which is determined by the bandwidth of the C-band MUX/DEMUX. Furthermore, the upstream pulse carriers generated from SC-BLS need to synchronize with the upstream data at ONUs.

To solve these problems, MLSE is proposed for upstream signal detection. Figure 2 depicts the analysis model of the proposed method. In the figure, the downstream link is omitted because it is not the bottleneck of the network and can be neglected. The SC spectrum is generated by feeding an optically amplified 1545 nm 3.5 ps 10 Gbit/s pulse train into a normal-dispersive dispersion-flattened fiber. The use of such kind of
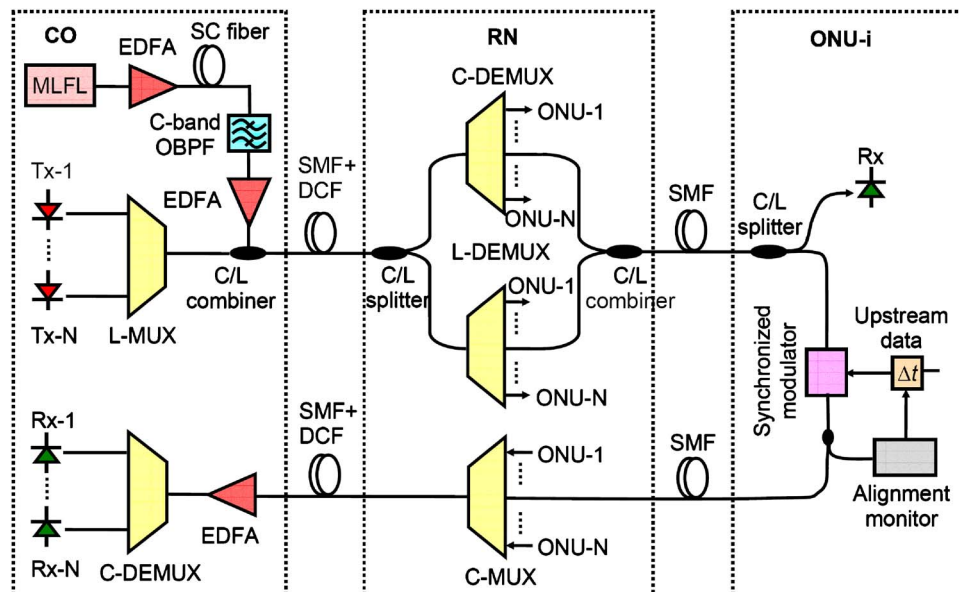
Fig. 1.   Architecture of SC-BLS WDM-PON.
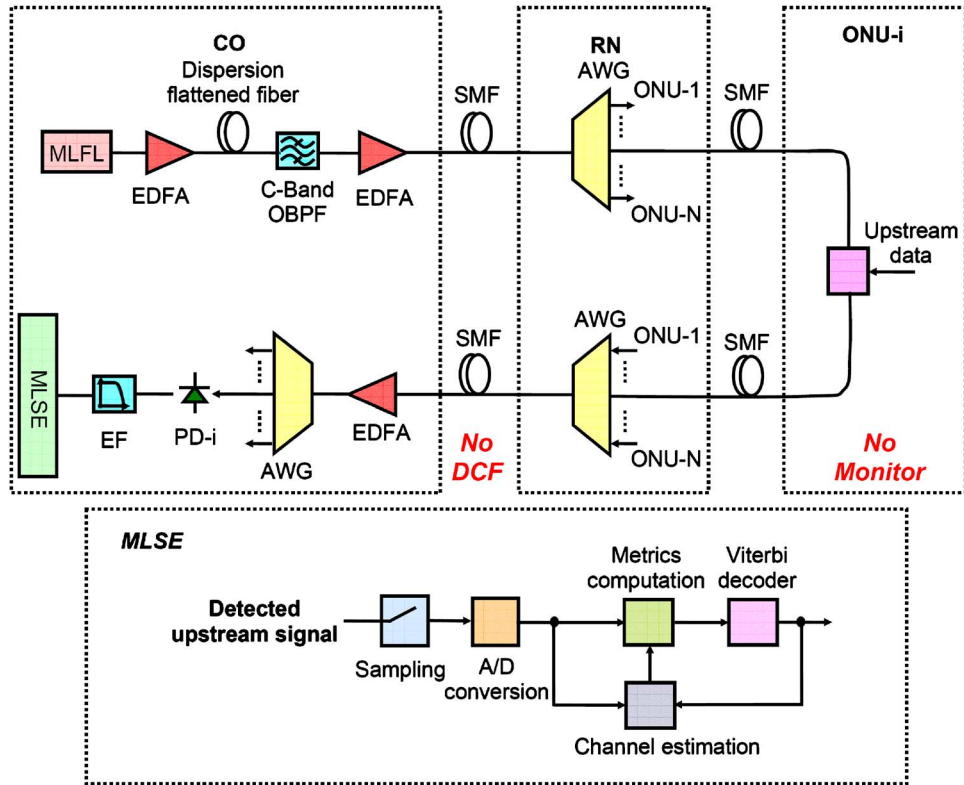
Fig. 2.   Analysis model of the proposed method.

fiber is essential to enable the SC generation with a flat and stable spectrum [8]. The pulse evolution in the SC fiber is governed by the following equation [9]:

$$\frac{\partial A(z,t)}{\partial z} + i\frac{\beta_2}{2}\frac{\partial^2 A(z,t)}{\partial t^2} = i\gamma|A(z,t)|^2 A(z,t), \tag{1}$$

where $A(z,t)$ is the slowly varying pulse envelope. The nonlinear coefficient γ and the group-velocity dispersion parameter β_2 are $2.2\,\text{W}^{-1}/\text{km}$ and $0.24\,\text{ps}^2/\text{km}$, respectively. Dispersion slope and fiber loss of the dispersion flattened fiber are negligible for practical consideration. The peak power of the optical pulses into the SC fiber, P, is 6 W. Split-step Fourier method is used to calculate Eq. (1). Figure 3(a) shows the 3 dB bandwidth of broadened SC spectrum versus SC fiber length. In the figure, the two spectral broadening processes are due to self-phase modulation (SPM) and four-wave mixing (FWM), respectively. $L_m = \rho(L_d L_n)^{1/2}$ in the figure denotes the fiber length when the spectral width reaches its first maximum, where the dispersion length L_d is T_0^2/β_2 and the nonlinear length L_n is $1/(\gamma P)$ [8]. T_0 is the input pulse width; ρ is a propor-
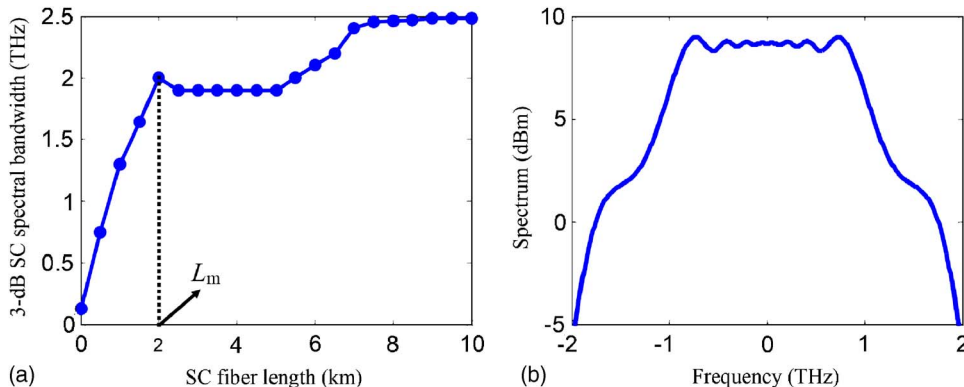
Fig. 3.   (a) Three decibel bandwidth of broadened SC spectrum versus SC fiber length. (b) Spectral profile at $L=3$ km.

tional factor and is pulse-shape dependent. To achieve optimal SC spectrum in terms of broadened SC spectral bandwidth and sliced upstream pulse quality, the SC fiber length L is chosen to be $L_m < L = 3$ km $< 2L_m$ [8]. Figure 3(b) shows the spectral profile at $L = 3$ km. From the figure, it is shown that a slight power fluctuation is exhibited for the SC spectrum from −800 to 800 GHz, which will lead to different sliced power for different channels as discussed later.

In the transmission link of the proposed scheme (Fig. 2), all fiber sections, feeder fibers CO-to-RN and RN-to-CO, and distribution fibers RN-to-ONUs and ONUs-to-RN, have no CD compensation. The CD of the SMF at 1545 nm is assumed to be 16 ps/km/nm. The SC spectrum is sliced into 16 channels with 100 GHz channel spacing by an AWG at RN. The bandwidth of the AWG determines the spectral width, thus the CD tolerance, of the sliced upstream channels. In the paper, two types of AWGs are used for investigation: (1) Gaussian-shaped AWG with 35 GHz 3 dB bandwidth and (2) second-order Gaussian-shaped AWG with 50 GHz 3 dB bandwidth. The sliced upstream carriers are modulated by modulators at ONUs without alignment monitors. The modulated signals are multiplexed at RN and sent back to CO.

At CO, the upstream signals are demultiplexed for detection. The detected signals are filtered by 7 GHz fourth-order Bessel electronic filters (EFs), sampled, analog-to-digital (A/D) converted, and equalized by MLSE. The metric of MLSE, $PM(a_n)$, is

$$PM(a_n) = PM(a_{n-1}) - \sum_j \log(p(I(t_j)|a_{n-m}, \ldots, a_n)). \tag{2}$$

For one sample per bit, $j = n - m/2$. For two samples per bit, $j = n - m/2$ or $n + 1/2 - m/2$. a_n and $p(I(t_j)|a_{n-m}, \ldots, a_n)$ are the nth upstream logical data and the probability of the sampled upstream signal value at time t_j given the logical data $a_{n-m}, \ldots, a_n$, respectively; m is the memory length and is assumed to be 4. Assuming that in the sequence estimation using the Viterbi algorithm, the estimated path $(b_0 \ b_1 \cdots b_{n-1} \ b_n)$ diverges from the correct path $(a_0 \ a_1 \cdots a_{n-1} \ a_n)$ at state k and remerges with the correct path at state $k + L$. Define two vectors to evaluate the error event in the estimation as $\varepsilon_c = [a_{k-m} a_{k-m+1} \cdots a_{k+L-2} a_{k+L-1}]$ and $\varepsilon_e = [b_{k-m} b_{k-m+1} \cdots b_{k+L-2} b_{k+L-1}]$. The bit error rate (BER) of MLSE is

$$P_e = \sum_{\varepsilon_c \neq \varepsilon_e} P(\varepsilon_c \to \varepsilon_e) w(\varepsilon_c, \varepsilon_e) \left(\frac{1}{2}\right)^{L+m}, \tag{3}$$

where $(\varepsilon_c \to \varepsilon_e)$ is the probability of the error event of transmitting ε_c but receiving ε_e. $w(\varepsilon_c, \varepsilon_e)$ is the number of nonzero components in the vector of $[(b_k - a_k)(b_{k+1} - a_{k+1}) \cdots (b_{k+L-m-1} - a_{k+L-m-1})]^T$.

The power budget for the upstream signals in Fig. 2 can be calculated. We find that the loss from the spectrum slicing is around 18 dB and 16 dB for 35 GHz Gaussian-shaped AWG and 50 GHz second-order Gaussian-shaped AWG, respectively. Assume that the output power of the SC-BLS from the CO, the fiber loss, the feeder-fiber length, the distribution-fiber length, and the insertion loss of the AWGs are 30 dBm, 0.2 dB/km, 20 km, 10 km, and 5 dB, respectively. The optical power entering the ONUs can be calculated to be 1 and 3 dBm for 35 GHz Gaussian-shaped AWG and 50 GHz second-order Gaussian-shaped AWG, respectively. We further assume that the loss for modulation at ONUs is 9 dB. Therefore, the power of the upstream signals before detection is calculated to be −26 and −23 dBm for these two AWGs, respectively. Since the receiver sensitivity with preamplification is −38 dBm at 10 Gbit/s [3], there is more than a 10 dB power margin for both AWGs. Note that compared to the conventional method using alignment monitors at ONUs and DCFs for CD compensation, the proposed method has an approximately 8 dB power saving.

Because for a fixed SC-BLS output power, the received power of the upstream signals varies for different channels and different types of AWGs. Therefore, the performance is evaluated in terms of the SC-BLS output power penalty rather than the received upstream signal power penalty. The SC-BLS output power penalty is with respect to the required SC-BLS output power for the ninth upstream channel to achieve a BER of 10^{-9} in the absence of asynchronous modulation and CD under 50 GHz second-order Gaussian-shaped AWG. The BER is obtained by using a semi-analytical calculation from Eq. (3). The stochastic noise is analytically calculated and

the deterministic effects, including SC generation in the dispersion-flattened fiber, CD in the SMF, optical filtering in the AWGs, and asynchronous upstream modulation at ONUs, are numerically calculated.

3. MLSE for Asynchronous-Modulation Compensation

First, the performance of MLSE to compensate asynchronous modulation of upstream pulse carriers is investigated. Figure 4 depicts the SC-BLS power penalty (dB) versus misaligned time for the ninth upstream channel by using conventional optimal threshold detection (solid curve) and one-sample per bit MLSE with the sampling phase at the center of eyes (dashed). Triangles and circles represent 35 GHz Gaussian-shaped AWG and 50 GHz second-order Gaussian-shaped AWG, respectively. Insets show the eye diagrams of the upstream signal under 35 GHz Gaussian-shaped AWG when the misaligned time is 0 and 50 ps. In the figure, feeder-fiber length and distribution-fiber length are assumed to be 0 km. From the figure, it is shown that when the misaligned time is 0 ps, 35 GHz Gaussian-shaped AWG (triangles) has ~3.2 dB SC-BLS power penalty increase compared to 50 GHz second-order Gaussian-shaped AWG (circles). It is because for 35 GHz Gaussian-shaped AWG, larger SC-BLS power is required to compensate the larger power loss from narrower-band optical spectrum slicing. When the upstream pulse carriers and the upstream data are not synchronized, the modulated upstream signals are highly degraded under conventional optimal threshold detection irrespective of the types of AWGs. For the misaligned time of −50 or 50 ps, the eyes are completely closed due to intersymbol interference (ISI), as shown in the insets of Fig. 4. By employing MLSE, however, the penalty is largely reduced. For misaligned time of −50 or 50 ps, the SC-BLS power penalties are bounded by 4.8 and 1.6 dB for 35 GHz Gaussian-shaped AWG and 50 GHz second-order Gaussian-shaped AWG, respectively. Notice that for 35 GHz Gaussian-shaped AWG, the penalty caused by asynchronous modulation is also 4.8 −3.2=1.6 dB. These results can be interpreted as follows. In the absence of CD, the impairment from asynchronous modulation is generalized as ISI with memory length $m \le 2$. We can derive the BER of one-sample per bit MLSE from Eq. (3) as
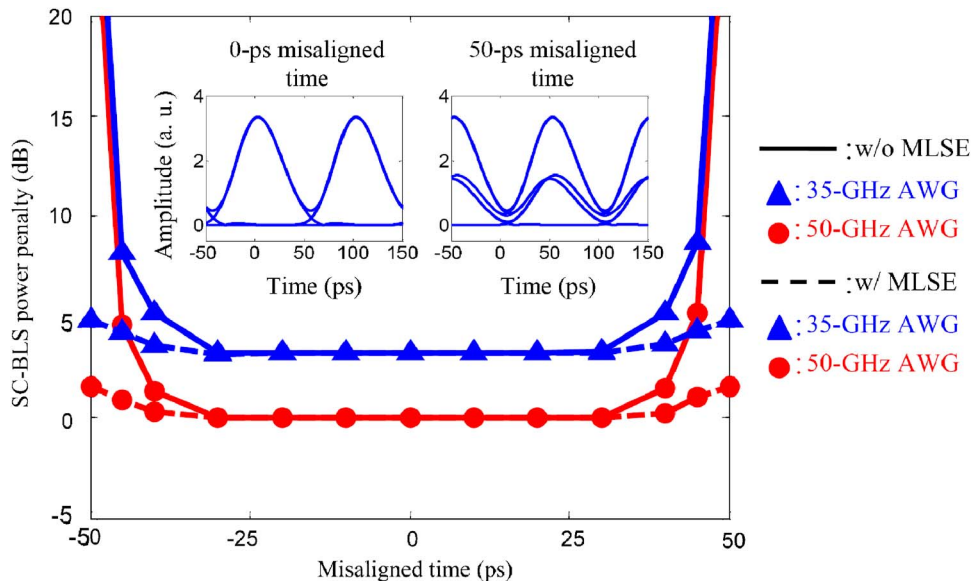
Fig. 4.   SC-BLS power penalty (dB) versus misaligned time for the ninth upstream channel by using conventional optimal threshold detection (solid) and one-sample per bit MLSE (dashed). Triangles and circles represent 35 GHz Gaussian-shaped AWG and 50 GHz second-order Gaussian-shaped AWG, respectively. Insets show the eye diagrams of the upstream signal under 35 GHz Gaussian-shaped AWG when the misaligned time is 0 and 50 ps.

$$P_e \approx Q\left(\left(\frac{f(0,0,1)^2 + f(0,1,0)^2 + f(1,0,0)^2}{2N_0}\right)^{1/2}\right) + \sum_{L=4}^{+\infty} (L-2)$$

$$\times \left(\frac{1}{2}\right)^{L-3} Q\left(\left(\frac{f(0,0,1)^2 + (f(0,0,1) - f(0,1,0))^2}{2N_0}\right.\right.$$

$$+ \frac{(L-4)(f(0,1,0) - f(1,0,1))^2 + (f(1,0,0) - f(0,1,0))^2 + f(1,0,0)^2}{2N_0}\left.\left.\right)^{1/2}\right), \qquad (4)$$

where $Q(x)$ is defined as the probability that a standard normal random variable exceeds x:

$$Q(x) = \int_x^{+\infty} \frac{e^{-y^2/2}}{(2\pi)^{1/2}} \mathrm{d}y. \qquad (5)$$

$f(p,q,r)$ in Eq. (4), $p,q,r \in \{0,1\}$, is the sampled signal value given the prior, the present, and the posterior upstream logical data of p, q, and r, respectively. N_0 is the noise power spectral density. For synchronized upstream modulation, $f(0,1,0) = f(1,1,1), f(1,0,0) = f(0,0,1) = f(1,0,1) = 0$. Therefore, Eq. (4) can be written as

$$P_e \approx Q\left(\left(\frac{f(1,1,1)^2}{2N_0}\right)^{1/2}\right) + \sum_{L=4}^{+\infty} (L-2)\left(\frac{1}{2}\right)^{L-3} Q\left(\left(\frac{(L-2)f(1,1,1)^2}{2N_0}\right)^{1/2}\right)$$

$$\approx Q\left(\left(\frac{f(1,1,1)^2}{2N_0}\right)^{1/2}\right), \qquad (6)$$

where the second "$\approx$" is satisfied because $Q(((L-2)f(1,1,1)^2/(2N_0))^{1/2})$, $L \geq 4$, is much smaller than $Q((f(1,1,1)^2/(2N_0))^{1/2})$ and can be neglected. For misaligned time of $-50\,\mathrm{ps}$, $f(1,0,1) = f(0,1,0) = f(1,0,0) = f(1,1,1)/2$, $f(0,0,1) = 0$. For misaligned time of $50\,\mathrm{ps}$, $f(1,0,1) = f(0,1,0) = f(0,0,1) = f(1,1,1)/2$, $f(1,0,0) = 0$. Therefore, in these two cases, Eq. (4) can be written as

$$P_e \approx Q\left(\left(\frac{f(1,1,1)^2}{4N_0}\right)^{1/2}\right) + \sum_{L=4}^{+\infty} (L-2)\left(\frac{1}{2}\right)^{L-3} Q\left(\left(\frac{f(1,1,1)^2}{4N_0}\right)^{1/2}\right) = 4Q\left(\left(\frac{f(1,1,1)^2}{4N_0}\right)^{1/2}\right).$$

$$(7)$$

From Eqs. (6) and (7), the penalty caused by asynchronous modulation can be found to be 1.6 dB. Although the result is obtained under one sample per bit, additional calculation shows that the increase of sample number per bit cannot improve the MLSE's performance. It is because the energy of the upstream return-to-zero (RZ) signals is concentrated at the center of eyes and additional sample between eyes is unable to provide more information.

Figure 5 shows the SC-BLS power penalty (dB) by using two-sample per bit MLSE for 16 upstream channels when the misaligned time is 50 ps. Triangles and circles represent 35 GHz Gaussian-shaped AWG and 50 GHz second-order Gaussian-shaped AWG, respectively. From the figure, it is shown that the power penalty varies with the upstream channels irrespective of the types of AWGs. However, such variation is due to the different sliced power from SC-BLS for different channels, as shown in Fig. 3(b). Additional results show that the penalty caused by asynchronous modulation is independent of the upstream channels as well as the types of AWGs and is bounded by 1.6 dB.

4. MLSE for CD Compensation

Figure 6(a) shows the SC-BLS power penalty (dB) versus the feeder-fiber length for the ninth upstream channel by using conventional optimal threshold detection (circles), one-sample per bit MLSE with the sampling phase at the center of the bit slot (triangles), one-sample per bit MLSE with the sampling phase between the bit slot (squares), and two-sample per bit MLSE (diamonds). In the figure, 50 GHz second-order Gaussian-shaped AWG and 0 km distribution-fiber length are assumed. From the figure, it is shown that the penalty increases rapidly under optimal thresh-
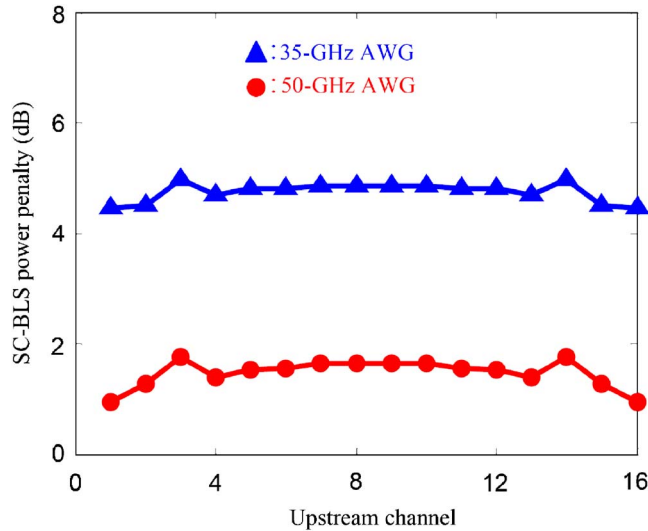
Fig. 5.   SC-BLS power penalty (dB) by using two-sample per bit MLSE for 16 upstream channels when the misaligned time is 50 ps. Triangles and circles present 35 GHz Gaussian-shaped and 50 GHz second-order Gaussian-shaped AWGs, respectively.

old detection (circles). For one-sample per bit MLSE (triangles and squares), when the feeder-fiber length is less than 15 km, the optimal sampling phase is at the center of the bit slot. One-sample per bit MLSE with optimal sampling phase provides limited performance improvement compared to optimal threshold detection. It is because for short feeder-fiber length, CD does not broaden the RZ pulses to the adjacent bits and cause ISI. The SC-BLS power penalty of the upstream signals is mainly from the pulses' peak power reduction.

In contrast, when the feeder-fiber length is larger than 15 km, CD-induced pulse broadening transfers the pulse energy from the center of the bit slot to the edge of the bit slot or even the adjacent bits. Therefore, the performance of MLSE with the sampling phase between eyes is comparable to that with the sampling phase at the center of the eyes. One-sample per bit MLSE with optimal sampling phase can largely reduce the SC-BLS power penalty. By using two-sample per bit MLSE, the CD tolerance of the upstream signals is further improved. The SC-BLS power penalty for 30 km feeder-fiber length is limited to around 3.6 dB.

To investigate the effects of AWGs on the CD tolerance of the upstream signals, Fig. 6(b) shows the SC-BLS power penalty (dB) versus the feeder-fiber length for the ninth upstream channel by using conventional optimal threshold detection (solid) and two-
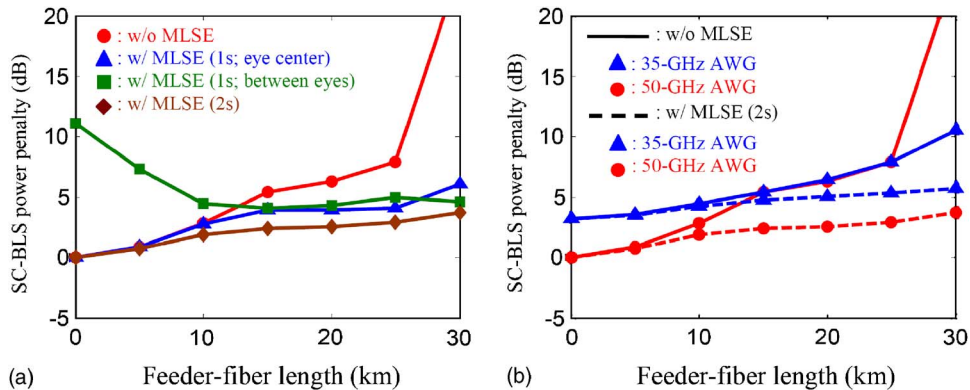
Fig. 6.   (a) SC-BLS power penalty (dB) versus the feeder-fiber length for the ninth upstream channel by using conventional optimal threshold detection (circles), one-sample per bit MLSE with the sampling phase at the center of the bit slot (triangles), one-sample per bit MLSE with the sampling phase between the bit slot (squares), and two-sample per bit MLSE (diamonds). (b) SC-BLS power penalty (dB) versus the feeder-fiber length for the ninth upstream channel by using conventional optimal threshold detection (solid) and two-sample per bit MLSE (dashed) when the AWG is Gaussian shaped with 35 GHz bandwidth (triangles) and second-order Gaussian shaped with 50 GHz bandwidth (circles).

sample per bit MLSE (dashed) when the AWG is Gaussian-shaped with 35 GHz bandwidth (triangles) and second-order Gaussian-shaped with 50 GHz bandwidth (circles). The distribution-fiber length is assumed to be 0 km. From the figure, it is shown that without MLSE (solid), despite its 3.2 dB back-to-back penalty increase, 35 GHz Gaussian-shaped AWG has comparable or better CD tolerance compared to 50 GHz second-order Gaussian-shaped AWG when the feeder-fiber length is larger than 15 km. It is because by using 35 GHz Gaussian-shaped AWG, the sliced upstream channels have narrower spectral bandwidth, resulting in better CD tolerance. By using MLSE, the penalty is largely reduced irrespective of the types of AWGs. At a feeder-fiber length of 30 km, the SC-BLS power penalties caused by CD under two-sample per bit MLSE are approximately $5.7 - 3.2 = 2.5$ dB and 3.6 dB for 35 GHz Gaussian-shaped AWG and 50 GHz second-order Gaussian-shaped AWG, respectively.

Figure 7 depicts the SC-BLS power penalty (dB) by using two-sample per bit MLSE for 16 upstream channels when the feeder-fiber length is 30 km. Triangles and circles present 35 GHz Gaussian-shaped AWG and 50 GHz second-order Gaussian-shaped AWG, respectively. From the figure, it is shown that similar to Fig. 5, the SC-BLS power penalty varies with different upstream channels regardless of the types of AWGs. However, such variation is due to the different sliced power from SC-BLS for different channels. The penalties caused by CD are channel independent and bounded by 2.5 and 3.6 dB for 35 GHz Gaussian-shaped AWG and 50 GHz second-order Gaussian-shaped AWG, respectively.

5. MLSE for Simultaneous Asynchronous-Modulation and CD Compensation

Next, an SC-BLS WDM-PON with feeder-fiber length of 20 km and distribution-fiber length ranging from 0 to 10 km is investigated. Figure 8 shows the SC-BLS power penalty (dB) versus misaligned time for the ninth upstream channel by using optimal threshold detection (solid curve) and two-sample per bit MLSE (dashed curve) when the AWG is (a) Gaussian-shaped with 35 GHz bandwidth; (b) second-order Gaussian-shaped with 50 GHz bandwidth. Circles, triangles, and squares represent the distribution-fiber length of 0, 5, and 10 km, respectively. In Fig. 8(b), the curve for 10 km distribution-fiber length and by using optimal threshold detection is not plotted due to its SC-BLS power penalty larger than 20 dB, as shown in Fig. 6. From Figs. 8(a) and 8(b) it is shown that under optimal threshold detection (solid), the SC-BLS power penalty increases dramatically for asynchronous upstream modulation irrespective of the types of AWGs. The increase of distribution-fiber length also leads to the increase of the SC-BLS power penalty. By using MLSE (dashed), the penalty is largely reduced. To facilitate the description, we define a maximal SC-BLS power pen-
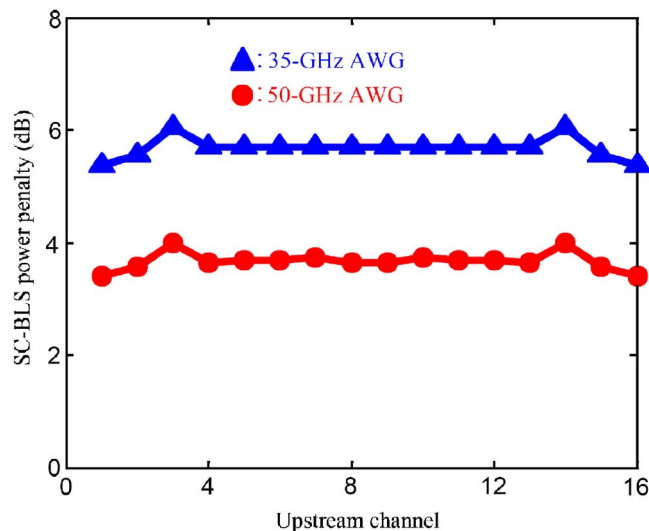
Fig. 7. SC-BLS power penalty (dB) by using two-sample per bit MLSE for 16 upstream channels when the feeder-fiber length is 30 km. Triangles and circles present 35 GHz Gaussian-shaped AWG and 50 GHz second-order Gaussian-shaped AWG, respectively.
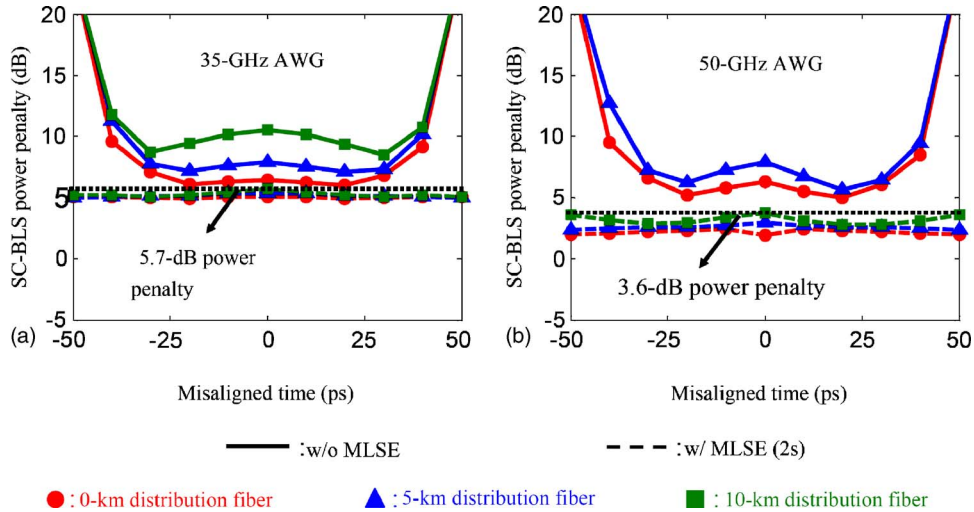
Fig. 8.   SC-BLS power penalty (dB) versus misaligned time for the ninth upstream channel by using optimal threshold detection (solid) and two-sample per bit MLSE (dashed) when the AWG is (a) Gaussian shaped with 35 GHz bandwidth; (b) second-order Gaussian shaped with 50 GHz bandwidth. Circles, triangles, and squares represent the distribution-fiber length of 0, 5, and 10 km, respectively.

alty, which is the maximal SC-BLS power penalty for varying misaligned time and distribution-fiber length. From Fig. 8, it is shown that the maximal SC-BLS power penalties by using two-sample per bit MLSE are bounded by 5.7 and 3.6 dB for 35 GHz Gaussian-shaped AWG and 50 GHz second-order Gaussian-shaped AWG, respectively. Note that for 35 GHz Gaussian-shaped AWG, there is 3.2 dB back-to-back penalty. Therefore, the penalty caused by asynchronous modulation and CD is 5.7 − 3.2 = 2.5 dB. From Fig. 8, it is also found that under MLSE detection (dashed), the penalty for asynchronous modulation is comparable to or even smaller than that for synchronized modulation irrespective of the types of AWGs. Such phenomenon is caused by the presence of CD and can be interpreted by Fig. 9.

Figure 9 depicts the upstream signal evolution for 50 ps misaligned time; (a) and (b) represent the cases in the absence of CD, i.e., feeder-fiber and distribution-fiber lengths of 0 km, and in the presence of CD, respectively. In (a), the pulse center is at the edge of the upstream data bit slot. Thus ISI is induced after upstream modulation. In (b), the CD in the fiber sections CO-to-RN and RN-to-ONUs introduces chirps to the upstream pulses, with positive frequency at the leading edge and negative frequency at the trailing edge. As a result, when the pulses are modulated at ONUs and transmitted back to CO through the fiber section ONUs-to-RN and RN-to-CO, not only pulse broadening effect but also pulse shifting effect are exhibited. The energy of the pulse shifts to the bit slot center, which alleviates ISI.

To evaluate the performance of MLSE for a different upstream channel detection, Fig. 10 depicts the maximal SC-BLS power penalty (dB) by using two-sample per bit MLSE for 16 upstream channels. Triangles and circles present 35 GHz Gaussian-
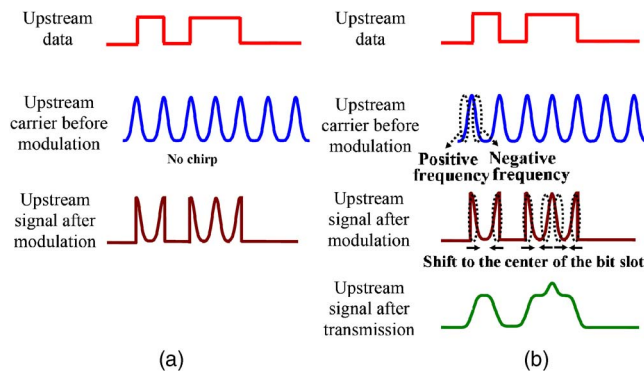
Fig. 9.   Upstream signal evolution for 50 ps misaligned time. (a) and (b) represent the cases without and with CD, respectively.
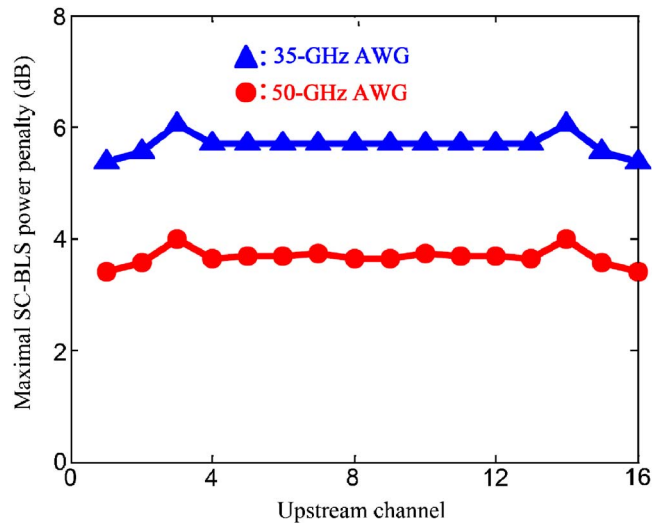
Fig. 10.   Maximal SC-BLS power penalty (dB) by using two-sample per bit MLSE for 16 up-stream channels. Triangles and circles present 35 GHz Gaussian-shaped AWG and 50 GHz second-order Gaussian-shaped AWG, respectively.

shaped AWG and 50 GHz second-order Gaussian-shaped AWG, respectively. Consider-ing the facts (1) different channels have different sliced power from SC-BLS; (2) there is 3.2 dB back-to-back penalty for 35 GHz Gaussian-shaped AWG, we can conclude from Fig. 10 that the maximal SC-BLS power penalties caused by asynchronous modulation and CD are channel independent and are bounded by 2.5 and 3.6 dB for 35 GHz Gaussian-shaped AWG and 50 GHz second-order Gaussian-shaped AWG, respectively.

6. Conclusions

We have proposed MLSE for 10 Gbit/s upstream signal detection to compensate asyn-chronous upstream modulation at ONUs and CD in the fibers in a SC-BLS WDM-PON. Analytical calculations show that MLSE bounds the penalty from asynchronous modulation by 1.6 dB for all upstream channels and different types of channel-slicing AWGs. We have investigated a 10 Gbit/s SC-BLS WDM-PON with feeder-fiber length of 20 km and distribution-fiber length ranging from 0 to 10 km. We show that irrespec-tive of the variation of distribution-fiber length, MLSE enables 10 Gbit/s upstream data transmission, with penalties caused by asynchronous modulation and CD bounded by 2.5 and 3.6 dB for 35 GHz Gaussian-shaped and 50 GHz second-order Gaussian-shaped channel-slicing AWGs, respectively. By eliminating alignment moni-tors at ONUs and all-optical CD compensation components, such technique features significant cost saving, lower power requirement for upstream signals, and lower operation complexity for ONUs in a SC-BLS WDM-PON.

Acknowledgments

References

1. K. Akimoto, J.-i. Kani, M. Teshima, and K. Iwatsuki, "Gigabit WDM-PON system using spectrum-slicing technologies," in *European Conference on Optical Communications* (IEEE, 2003), paper Th2.4.6.
2. E. Wong, K. L. Lee, and T. B. Anderson, "Directly modulated self-seeding reflective semiconductor optical amplifiers as colorless transmitters in wavelength division multiplexed passive optical networks," J. Lightwave Technol. **25**, 67–74 (2007).
3. B. Zhang, C. Lin, L. Huo, Z. Wang, and C.-K. Chan, "A simple high-speed WDM PON utilizing a centralized supercontinuum broadband light source for colorless ONUs," in *Optical Fiber Communication Conference and Exposition and The National Fiber Optic Engineers Conference*, Technical Digest (CD) (Optical Society of America, 2006), paper OTuC6. http://www.opticsinfobase.org/abstract.cfm?URI=OFC-2006-OTuC6
4. H. Takara, "Supercontinuum multi-carrier source for WDM systems," in *Optical Fiber*

Communication Conference, A. Sawchuk, ed., Vol. 70 of OSA Trends in Optics and Photonics (Optical Society of America, 2002), paper WR5. http://www.opticsinfobase.org/abstract.cfm?URI=OFC-2002-WR5

5. H. Bulow, "Electronic dispersion compensation," in *Proceedings of the Optical Fiber Communication Conference* (Optical Society of America, 2007), paper OMG5.

6. X. Liu and X. Wei, "Electronic dispersion compensation based on optical field reconstruction with orthogonal differential direct-detection and digital signal processing," in *Proceedings of the Optical Fiber Communication Conference* (Optical Society of America, 2007), paper OTuA6.

7. A. Farbert, S. Langenbach, N. Stojanovic, C. Dorschky, T. Kupfer, C. Schulien, J.-P. Elbers, H. Wernz, H. Griesser, and C. Glingener, "Performance of a 10.7 Gb/s receiver with digital equaliser using maximum likelihood sequence estimation," in *European Conference on Optical Communication* (2004), paper Th4.1.5.

8. S. Taccheo and K. Ennser, "Investigation of amplitude noise and timing jitter of supercontinuum spectrum-sliced pulses," IEEE Photon. Technol. Lett. **14**, 1100–1102 (2002).

9. G. P. Agrawal, *Nonlinear Fiber Optics*, 3rd. ed. (Academic, 2001).